Radical Production and Kinetic Procedure. Arsanyl radicals were generated in the cavity of a Varian E-3 epr spectrometer by photolysis (using a 200-W Osram super pressure mercury lamp) of deoxygenated solutions of the appropriate tertiary arsine (0.01–0.1 *M*) and di-*tert*-butyl peroxide in a low-boiling solvent (typically isopentane, trichlorofluoromethane, or toluene). Some of the runs were carried out in the presence of phenyl *N*-*tert*-butyl nitrone (0.001 *M*). Reaction temperatures were varied between 0° and −120° with a Varian V-4557 variable-temperature accessory. Radical accumulations and decays were recorded with the *X*–*Y* recorder provided with the spectrometer or in a Fabri-Tek 1072 signal averager. The absolute concentration of an arsanyl radical was determined by comparing the double integration (×4) of one of the first derivative lines with the double integration (at the same temperature) given by a standard solution of 2,2-diphenyl-1-picrylhydrazyl.[17]

(17) (a) K. Adamic, J. A. Howard, and K. U. Ingold, *Can. J. Chem.*, **47**, 3803 (1969); (b) K. Adamic, D. F. Bowman, T. Gillan, and K. U. Ingold, *J. Amer. Chem. Soc.*, **93**, 902 (1971).

Decomposition of *tert*-Butyl Hyponitrite in the Presence of Some Tertiary Arsines. *tert*-Butyl hyponitrite and the appropriate arsine (either triphenylarsine, diphenylmethoxyarsine, diphenylethoxyarsine, or diphenyl-*tert*-butoxyarsine) were heated in deoxygenated isopentane or toluene at 50° for 10 half-lives of the hyponitrite. The volatile reaction products were analyzed by glc and mass spectroscopy, while the involatile products were analyzed by infrared spectroscopy. The principal volatile reaction products produced from these reactions are summarized in Table III.

Relative Reactivities of Triphenylarsine and Triethyl Phosphite to *tert*-Butoxy Radicals. A mixture of triphenylarsine (0.003 *M*) and triethyl phosphite (0.005 *M*) in deoxygenated trichlorofluoromethane containing di-*tert*-butyl peroxide was photolyzed *in situ* in the cavity of the spectrometer. Rates of accumulation and steady-state concentrations of $(EtO)_3\dot{P}OB$ and $Ph_3\dot{A}sOB$ were measured and gave the relative reactivities of the two substrates toward *tert*-butoxy radicals.

Acknowledgment. One of us (E. F.) thanks the Chevron Research Company for financial support in the form of a fellowship.

Electronic Spectra of Ruthenium and Osmium Tetroxides

S. Foster, S. Felps, L. W. Johnson, D. B. Larson, and S. P. McGlynn*

Contribution from The Coates Chemical Laboratories, The Louisiana State University, Baton Rouge, Louisiana 70803. *Received April 4, 1973*

Abstract: The electronic absorption spectra of gaseous ruthenium and osmium tetroxides have been measured in the energy region below 11 eV and the two lowest energy band systems of both materials have been investigated in SF_6 matrices at temperatures down to 20°K. It is shown that the substructure in the two initial band systems is vibronic, (*i.e.*, ν_2(e) activity). It is also shown that the electronic spectrum can be subdivided into valence and Rydberg bands and that much of the spectrum is interpretable using pes data. The relative energy of the virtual 2e-MO in RuO_4 and OsO_4 has been determined and it is the lesser antibonding energy of this MO in RuO_4 which is responsible for the lower energy of the valence transitions of this material.

The purpose of this work is to elaborate the electronic absorption spectra of gaseous RuO_4 and OsO_4 in the range 5000–1000 Å and to attempt an analysis of these spectra using photoelectron spectroscopic (pes) data recently generated in these laboratories.[1]

The pes data are tabulated in Figure 1 and provide the energies of the five highest energy filled MO's. The lowest energy virtual MO's are also shown in Figure 1. We believe, based on computational data[1] as well as on intensity considerations of the five lowest energy transitions of RuO_4 and OsO_4, that the two lowest energy virtual MO's, in order of increasing energy, are 2e and $4t_2$. We also maintain, based on the analysis which will be given, that the 2e-MO of RuO_4 is approximately 1 eV less energetic than the 2e-MO of OsO_4 and that it is this fact which is largely responsible for the lower electronic transition energies found in RuO_4. Finally, based on a fitting of spectroscopic data, a fitting which is probably quite suspect, we think that the $4t_2$-MO's of RuO_4 and OsO_4 are nearly isoenergetic and ~3.5 eV higher than the 2e-MO of OsO_4. These prejudices are all elaborated in Figure 1 and will be discussed in the text. The only other virtual MO resulting from the basis set of AO's used in the computations (*i.e.*, the $3a_1$-MO) is situated in the continuum, is probably disruptive (if populated) of molecular integrity, and is not important to the discussion of spectroscopic characteristics; this MO is not shown in Figure 1.

(1) S. I. Foster, S. Felps, L. C. Cusachs, and S. P. McGlynn, *J. Amer. Chem. Soc.*, submitted for publication.

The virtual AO's of metal and oxygen which were not included in the AO computational basis set are used in a discussion of the higher energy region of the spectrum. The virtual AO's of the metal are not needed for this purpose since they lie at considerably higher energies than the virtual AO's of the oxygens. In other words, all of the higher energy electronic spectroscopy can be rationalized in terms of Rydberg transitions from filled MO's of the ground state to virtual oxygen-like pseudo-AO's. Since these pseudo-AO's have approximately the same energy in both molecules and since the filled MO's of Figure 1 are also quite similar energetically, it follows that the Rydberg transitions, in contrast to the valence transitions, should be more or less isoenergetic. It is this premise, namely the dominance of Rydberg transitions, which is responsible for the energy coincidence of many features of both spectra in their high-energy regions.

Any discussion which attempts to discuss state energy differences, whether obtained from pes or simple electronic absorption spectroscopy data, in terms of MO energies is clearly dangerous. That course, without apology, is the tack which this discussion will adopt.

Experimental Section

Ruthenium and osmium tetroxide (Alfa Inorganics) were purified by repeated freeze–evacuate–thaw cycles until all light gas contaminants were removed. Absorption spectra in the gas phase were recorded on Cary 14, Cary 15, and McPherson Model 225 spectrophotometers, double paths being employed in all instances. All gases were flowed continuously through the sampling cell during the course of measurements. This tactic evaded all difficulty with decomposition except for RuO_4 in the range 2000–1000 Å. The rate of decomposition of RuO_4 in this wavelength region was such that the flow rate had to be increased and the spectrum recorded feature by feature, sample cell windows being replaced as baseline requirements dictated.

Matrix isolated samples were prepared from a mixed gas 1/500 MO_4/SF_6 mol ratio and frozen on a cold surface in a Cryotip.[2] Thereafter, spectra were recorded at various temperatures down to 20°K.

Discussion

Bands I and II. The electronic spectra of gas-phase RuO_4 and OsO_4 are shown in Figures 2 and 3, respectively. The two lowest energy band systems, bands I and II, of both these compounds have been studied previously,[3] under higher resolution conditions than those available to us. Suffice it here, therefore, to state that in band I a rather long progression in a $\nu_1(a_1)$ frequency of 782 and 813 cm^{-1} is observed for RuO_4 and OsO_4, respectively, the corresponding ground-state frequencies[4,5] being 885.3 and 965.2 cm^{-1}. A complex substructure is also apparent in both bands, one of these being particularly pronounced in RuO_4 and separated from the main vibronic peaks by an average of 242 cm^{-1}. Band II also exhibits a long progression in a $\nu_1(a_1)$ frequency of 771 and 843 cm^{-1} in RuO_4 and OsO_4, respectively, as well as a complex substructure dominated by intervals of 250 (RuO_4) and 164 cm^{-1} (OsO_4) from the main vibronic peaks. This smaller splitting may result from vibronic activity in a non-totally symmetric vibrational mode, from a Jahn–Teller splitting such as is observed[1] for the $^2T_2$ ionic state of OsO_4, from "hot-band" activity, or from other electronic transitions which are partly occluded beneath the absorption envelope.

The point of this discussion relates to the matrix-isolation spectra of Figure 4 in which, despite some loss of resolution caused by deposition effects, the substructure of the gas-phase OsO_4 spectrum remains quite intact. It may be concluded, therefore, that the substructure is not of "hot-band" nature. Similarily, since bands I and II of RuO_4 red shift by 300 and 1600 cm^{-1}, respectively, on going to the solid state and those of OsO_4 red shift by 417 (1197) or 1100 (1850) cm^{-1}, where the numbers in parentheses denote a less probable choice of corresponding bands in the gaseous- and solid-state spectra, it would appear that different electronic states (including states produced by Jahn–Teller distortions) should differ considerably with regard to the energy shift experienced in going from gas to solid. It is clear from Figure 4 that the substructure of band II of OsO_4 retains its position relative to the main vibrational peaks and this, plus its apparent intensity diminution, lead us to classify this substructure as vibronic in nature. A similar conclusion follows from the RuO_4 studies; however, in this instance, it was band I which retained resolution in the solid phase. Hence, the dominant substructure of bands I and II almost certainly represents excited-state activity of a $\nu_2(e)$ ground-state frequency[4] of ~320 cm^{-1}.

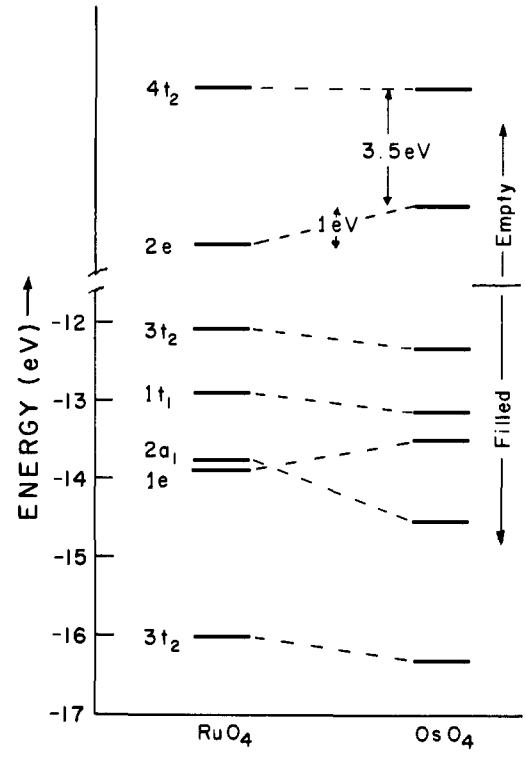

Figure 1. An MO energy level diagram based on experimental data.

The red shifts which occur in the solid phase indicate that the various excited states are more polarizable than the ground state, that for the terminal state of transition II being largest. These effects are undoubtedly associable with increased metal d orbital populations in the excited states.

Classification. The spectra of Figures 2 and 3 can be classified into two types: valence transitions and Rydberg transitions. The valence transitions correspond to excitation of valence shell electrons to either the 2e or $4t_2$ virtual molecular orbitals. The Rydberg transitions correspond to excitation of valence shell electrons to the set of pseudo-atomic oxygen-like orbitals 3s, 3p, 4s, etc., located on the oxygen centers; the excitation to pseudo-atomic orbitals located on the metal is expected to lie outside the upper energy range achieved in this work.

The molecular transitions are labeled I–VI in Figures 2 and 3. If the RuO_4 spectrum is shifted approximately 10,000 cm^{-1} toward higher energies, bands I–VI of both compounds become more or less coincident. On the other hand, since the lower ionization potentials of RuO_4 and OsO_4 are closely similar and since the pseudo-AO's on oxygen are presumably identical in both compounds, it follows that coresponding Rydberg transitions should be more or less isoenergetic in both compounds. Thus, those bands which are of Rydberg type should be almost coincident when the spectra are superposed according to the energy abscissa.

Molecular Transitions. The lowest energy virtual

(2) Air Products and Chemicals, Inc., Allentown, Pa. (Model AC-2-110).
(3) E. J. Wells, A. D. Jordan, D. S. Alderdice, and I. G. Ross, *Aust. J. Chem.*, **20**, 2315 (1967).
(4) R. McDowell and M. Goldblatt, *Inorg. Chem.*, **10**, 625 (1971).
(5) R. S. McDowell, L. B. Asprey, and L. C. Hoskins, *J. Chem. Phys.*, **56**, 5712 (1972).

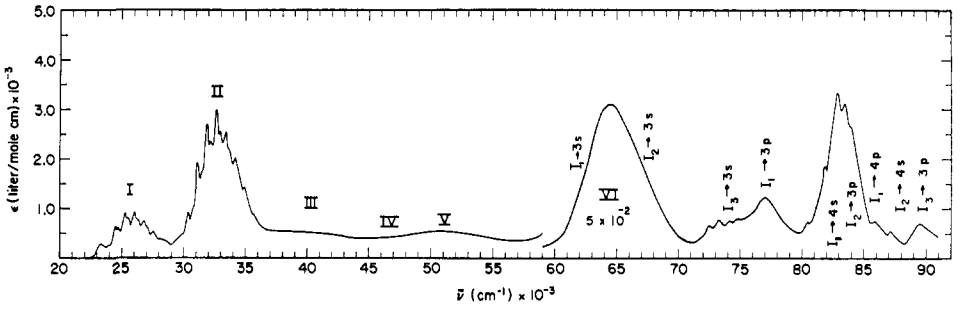

Figure 2. The gas-phase spectrum of RuO_4.

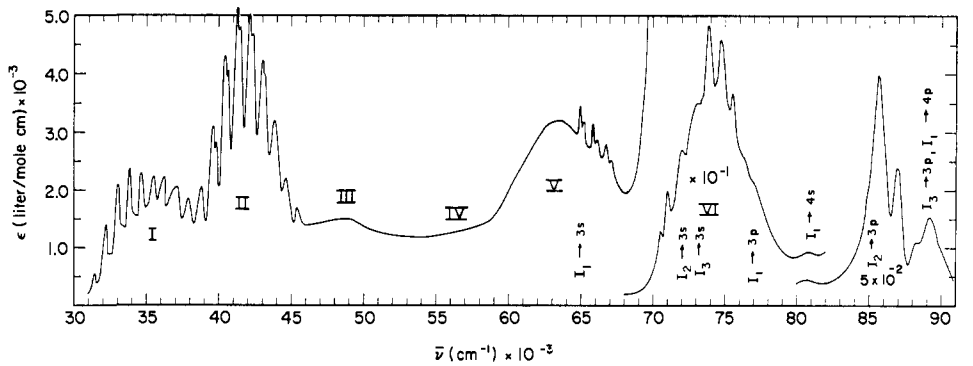

Figure 3. The gas-phase spectrum of OsO_4.

Table I. Analysis of Electronic Spectra of RuO_4 and OsO_4

Filled MO, i[a]	i → 2e,[b] cm^{-1}	i → $4t_2$,[b] cm^{-1}	i → R,[c] cm^{-1}	Obsd,[d] cm^{-1}	Band
		(a) RuO_4			
$3t_2$	≡26000 (A)			26000 (S)	I
$1t_1$	32600 (A)			33000 (S)	II
$2a_1$	39600 (F)			40600 (W)	III
1e	40400 (F)			45000 (W)	IV
$2t_2$	~58000 (A)			52000 (W)	V
$3t_2$			52000 (3s)	62000 (sh)	
$3t_2$		≡64500 (A)		64500 (S)	VI
$1t_1$			68000 (3s)	67000 (sh)	
$1t_1$, $2a_1$		71100 (A)	75000 (3s)	74000 (S)	
$2a_1$, $3t_2$		78100 (A)	78000 (3p)	77000 (S)	
1e		79000 (A)		80500 (W)	
$3t_2$			83000 (4s)	82000 (S)	
$1t_1$			84000 (3p)	83000 (S)	
$3t_2$			88000 (4p)	86000 (S)	
$1t_1$			89000 (4s)	87000 (S)	
$2a_1$			91000 (3p)	89500 (S)	
$2t_2$		~96500 (A)			
		(b) OsO_4			
$3t_2$	≡35000			35000 (S)	I
$1t_1$	41500			42000 (S)	II
1e	44500			48000 (W)	III
$2a_1$	52900			56000 (W)	IV
$2t_2$, $3t_2$	~67000 (A)	64000 (A)		64000 (S)	V
$3t_2$			64000 (3s)	65000 (W)	
$1t_1$, $1t_1$		70500 (A)	72000 (3s)	71000 (S)	
1e		73500 (A)		74000 (S)	VI
1e			73000 (3s)	74000 (S)	
$3t_2$			79000 (3p)	77000 (W)	
$3t_2$			85000 (4s)	81000 (W)	
$2a_1$		81900 (A)		85600 (S)	
$1t_1$			86000 (3p)	87000 (S)	
1e			89000 (3p)	88300 (S)	
$3t_2$			89000 (4p)	89000 (S)	
$2t_2$		~96000 (A)			

[a] When two i-MO's are listed, the order of listing is the serial order of appearance in columns 2–4. [b] The letters A and F in parentheses denote allowed and forbidden electric dipole transitions, respectively. [c] The symbols in parentheses represent the terminal Rydberg AO, R. [d] The symbols in parentheses denote intensities: strong (S); weak (W); shoulder (sh).

MO of tetrahedral tetroxides which are isoelectronic with MnO_4^- is generally supposed to be the 2e-MO. This is also the result of the computations reported[1] for OsO_4 and RuO_4. The only other accessible virtual MO is the $4t_2$-MO, and computations indicate that this MO is more energetic by approximately 18,000–25,000 cm^{-1} than the 2e-MO. Calculations on other isoelectronic tetroxides indicate 2e-$4t_2$ energy separations as large as 40,000 cm^{-1}. In view of this, and the close energy clumping of the valence shell MO's which is found by photoelectron spectroscopic studies (see Figure 1), it follows that the lower energy regions of the spectra of Figure 1 should represent transitions which terminate on the 2e-MO. Furthermore, since a number of the filled MO's have closely similar nature, it follows that many Coulomb and exchange integrals ought to be closely similar and that much of the molecular spectrum might be systematized using the pes data.

An effort to accomplish such a systematization is essayed in Table I. Given the energy of the $3t_2 \rightarrow 2e$ transition in OsO_4 as 35,000 cm^{-1} (*i.e.*, the energy of band I), it follows that the energies of the other transitions to the 2e-MO may be estimated from a knowledge of the ionization potentials. A similar attempt is essayed in Table I for RuO_4, with the $3t_2 \rightarrow 2e$ transition equated to 26,000 cm^{-1}. It follows that a similar attempt may be made for the $i \rightarrow 4t_2$ transition but that such an attempt may well founder on the fact that the energy of the $3t_2 \rightarrow 4t_2$ transition is not known. A "guess" at this energy is made in Table I. The basis of the guess is as follows. Band V in RuO_4 is much less intense than in OsO_4. We have made the assumption that the anomalous intensity of band V in OsO_4 is associated with the fact that it encompasses both the allowed transitions $2t_2 \rightarrow 2e$ and $3t_2 \rightarrow 4t_2$, whereas that of RuO_4 contains only the $2t_2 \rightarrow 2e$ excitation, the $3t_2 \rightarrow 4t_2$ excitation being retained for band VI of RuO_4.

Table II. The Energy Difference, ΔE_{2e}, between the 2e-MO's of OsO_4 and RuO_4 (Using the Relation $\Delta E_{2e} = \Delta(h\nu)_{i\rightarrow 2e} - \Delta I_i$)

Filled MO, i	i → 2e, eV OsO_4	i → 2e, eV RuO_4	ΔI_i, eV OsO_4 − RuO_4	ΔE_{2e}, eV
$3t_2$	4.34	3.22	+0.23	0.89
$1t_1$	5.21	4.09	+0.22	0.90
1e	5.95	5.58	+0.38	0.75
$2a_1$	6.94	5.03	−0.76	1.15
$2t_2$	7.93	6.45	+0.28	1.20
			Av	0.98

Granted that all five initial transitions terminate on the 2e-MO, it follows that $\Delta(h\nu)_{i\rightarrow 2e} - \Delta I_i = \Delta E_{2e}$: where ΔI_i is the difference in the ionization energy of the i-MO between OsO_4 and RuO_4; $\Delta(h\nu)$ and ΔE_{2e} are the corresponding differences in transition energies and 2e-MO energies between the same compounds. This equation is valid only when Coulomb repulsion and exchange terms are equal and when configuration interaction effects are small. An analysis of transitions I–IV is given along these lines in Table II. It would appear that the 2e-MO of OsO_4 is approximately 1 eV higher in energy in OsO_4 than in RuO_4 and that it is this factor which is dominantly responsible for the blue shift of the OsO_4 spectrum relative to that of RuO_4.

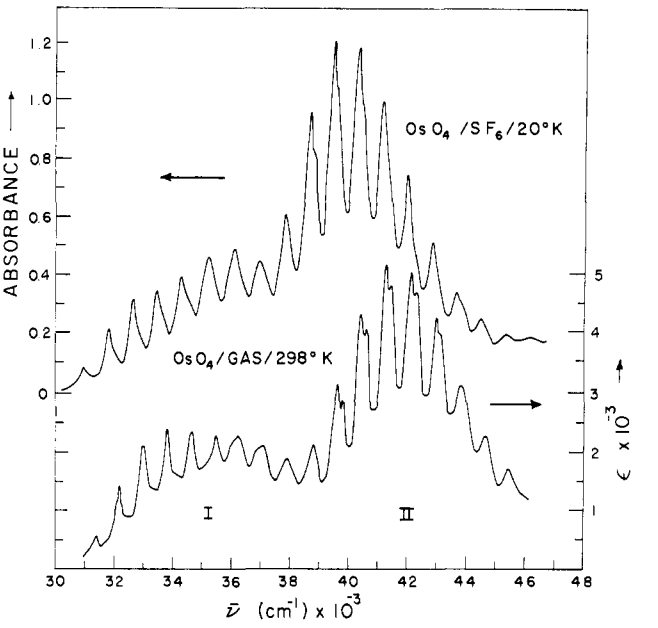

Figure 4. Gas-phase spectra (298 °K) and matrix-isolation spectra of OsO_4 (~1/500 molar dilution in SF_6 at ~20 °K).

It is rather more difficult to say anything conclusive about the energetic whereabouts of the $4t_2$-MO. Based on the assumptions made, the calculated $i \rightarrow 4t_2$ energies are those shown in Table I. They do happen to correspond to observed absorption bands, some of which are not otherwise assignable. Apart from this, the $3e–4t_2$ energy gap does appear to be rather large, particularly in RuO_4, and it seems best to view the quoted $4t_2$-MO energy as quite uncertain.

Finally, we note that the relative intensities of the first five bands, based on group-theoretical considerations of electric dipole allowedness, are in accord with that expected in OsO_4 but not in RuO_4.

Rydberg Spectra. It is our opinion that much of the higher energy structure in both spectra is of Rydberg nature. We base this conclusion on the following arguments.

(i) Recent work from these laboratories[6] has shown that an oxygen center which is bound to one other atom possesses low-energy Rydberg excitations which are not readily distinguishable from intravalence-shell transitions insofar as band shapes or intensities are concerned. In particular, the quantum defects for $N \rightarrow 3p(R)$ and $N \rightarrow 3s(R)$ on oxygen, where N is the ground state, were found to be 0.66 and 1.25, respectively, for molecules with ionization energies close to those of RuO_4 and OsO_4.

(ii) Knowing the various ionization energies, I, of the ground state, it follows that the Rydberg transition energies are calculable using $h\nu = I - R/(n+\delta)^2$ where n is the principal quantum number of the terminal oxygen atomic orbital and δ is the quantum defect. Such energies have been computed and are also compared with experiment in Table I. The agreement is remarkably good.

(iii) According to the analysis of Table I, the three peaks on the high-energy side of band V of OsO_4 correspond to the $3t_2 \rightarrow 3s(R)$ transition. As such,

(6) H. J. Maria, J. L. Meeks, P. Hochmann, J. R. Arnett, and S. P. McGlynn, *Chem. Phys. Lett.*, **19**, 309 (1973).

it is not surprising that the principal features of this band system are not unlike those in that part of the photoelectron spectrum which concerns ionization of the $3t_2$ electron: a progression in $\nu_1(a_1)$ of 840 cm^{-1} with a $\nu(e)$ or $\nu(t_2)$ vibronic substructure of $\sim$210 cm^{-1}. The $1t_1 \rightarrow 3s(R)$ transition corresponds to the structure on the low-energy side of band VI. It contains three peaks separated by $\sim$950 cm^{-1}, a $\nu_1(a_1)$ frequency not detectably different from that of the ground state at 965 cm^{-1}. The $1e \rightarrow 3s(R)$ transition corresponds to the three well-resolved peaks on top of band VI and consists of a progression in $\nu_1(a_1)$ of $\sim$870 cm^{-1}. Thus, in all transitions where vibrational structure is resolved, the band characteristics parallel those in the pes spectrum and we take this to indicate pseudo-ionic (*i.e.*, Rydberg) character.

The $3t_2 \rightarrow 3s$ and $1t_1 \rightarrow 3s$ Rydbergs are thought not to be resolved in RuO_4 and to lie within the compass of band VI. This is, perhaps, a convenient analysis but it is not inconsistent with the large half-width of this band or its large intensity.

Acknowledgment. The authors wish to express their gratitude to Hung-tai Wang and Petr Hochmann of these laboratories for considerable help with the Rydberg analysis. This work was supported by contract between the United States Atomic Energy Commission-Biology Branch and the Louisiana State University.

Electrogenerated Chemiluminescence. XIII. Electrochemical and Electrogenerated Chemiluminescence Studies of Ruthenium Chelates

Nurhan E. Tokel-Takvoryan, Ronald E. Hemingway, and Allen J. Bard*

Contribution from the Department of Chemistry, University of Texas, Austin, Texas 78712. *Received January 18, 1973*

Abstract: The electrochemistry and electrogenerated chemiluminescence (ecl) of four ruthenium(II) chelates, RuL_x^{n+} ($x = 3$, $n = 2$, L = 2,2′-bipyridine (bipy); $x = 3$, $n = 2$, L = 1,10-phenanthroline (*o*-phen); $x = 2$, $n = 2$, L = 2,2′,2″-terpyridine (terpy); $x = 2$, $n = 3$, L = 2,4,6-tripyridyl-*s*-triazine (TPTZ)), in acetonitrile solutions were investigated. All compounds showed evidence of several one-electron reduction and oxidation steps to form products stable during cyclic voltammetric scans. Coulometric and rotating ring-disk electrode (RRDE) studies of the bipy chelate were also carried out. The bipy, *o*-phen, and terpy chelates produce ecl *via* redox reactions of oxidized and reduced forms to form an emitting species, which has been identified as the triplet state by comparison to its luminescence spectrum; the ecl of the bipy chelate is the most intense. A study of ecl of the bipy chelate at the RRDE yielded an ecl efficiency of 5–6%.

The luminescence properties of a number of d^6 metal ions complexed to π-conjugated ligands have been reported. The second and third row transition d^6 metal complexes of Rh(III), Ir(III), Os(III), and Ru(II) display phosphorescence which is assigned to transitions which are "metal localized," (*i.e.*, $Rh(bipy)_2Cl_2^+$),[1,2] "ligand localized" ($Rh(o\text{-phen})_3^{3+}$),[3] and "charge transfer" in origin ($Ru(bipy)_3^{2+}$)[4,5] and ($Ir(bipy)_3^{3+}$).[6]

Previous reports of electrogenerated chemiluminescence (ecl) have demonstrated the generation of excited states by electrogenerated radical ion annihilation reactions of organic aromatic hydrocarbons and heterocyclic and macrocyclic[7] compounds in aprotic media. In a recent communication[8] we reported ecl obtained from the $Ru(bipy)_3Cl_2$ system in acetonitrile. We now wish to present the results of more detailed studies of the $Ru(bipy)_3^{2+}$ system and other $Ru(L)_x^{n+}$ systems in acetonitrile ($x = 3$, $n = 2$, L = 1,10-phenanthroline (*o*-phen); $x = 2$, $n = 2$, L = 2,2′,2″-terpyridine, (terpy); $x = 2$, $n = 3$, L = 2,4,6-tripyridyl-*s*-triazine, TPTZ).

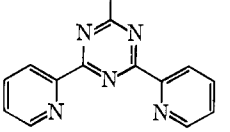

2,4,6-tripyridyl-*s*-triazine (TPTZ)

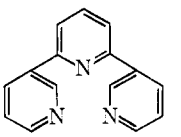

2,2′,2″-terpyridine (terpy)

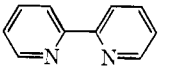

2,2′-bipyridine (bipy)

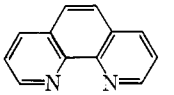

1,10-phenanthroline (*o*-phen)

Experimental Section

$Ru(bipy)_3Cl_2 \cdot 6H_2O$ and $Ru(o\text{-phen})_3Cl_2$ were purchased from G. F. Smith Chemical Co., and each was purified by triple recrys-

(1) G. A. Crosby and D. H. W. Carstens, "Molecular Luminescence," F. C. Lim, Ed., W. A. Benjamin, New York, N. Y., 1969, p 309.
(2) D. H. W. Carstens and G. A. Crosby, *J. Mol. Spectrosc.*, **34**, 113 (1970).
(3) M. K. DeArmond and J. E. Hillis, *J. Chem. Phys.*, **49**, 466 (1970).
(4) F. E. Lytle and D. M. Hercules, *J. Amer. Chem. Soc.*, **91**, 253 (1969).
(5) J. N. Demas and G. A. Crosby, *J. Mol. Spectrosc.*, **26**, 72 (1968).
(6) K. R. Wunschel, Jr., and W. E. Ohnesorge, *J. Amer. Chem. Soc.*, **89**, 2777 (1967).
(7) N. E. Tokel, C. P. Keszthelyi, and A. J. Bard, *J. Amer. Chem. Soc.*, **94**, 4872 (1972).
(8) N. E. Tokel and A. J. Bard, *J. Amer. Chem. Soc.*, **94**, 2862 (1972).